Supplementary Online Content

Zhao Q, Sullivan EV, Honnorat N, et al. Association of heavy drinking with deviant fiber tract development in frontal brain systems in young adolescents. *JAMA Psychiatry.* Published online December 30, 2020. doi:10.1001/jamapsychiatry.2020.4064

This supplementary material has been provided by the authors to give readers additional information about their work.

eMethods. Supplementary Methods

Data Matching. An age-sex-matched data set of no-to-low and heavy drinkers was created using the maximum bipartite matching algorithm [1, 2]. The method first constructed a bipartite graph such that the first set of nodes represented 291 no-to-low drinkers and the second set of nodes represented 160 heavy drinkers. An edge was connected between a no-to-low drinker and a heavy drinker if they were of the same gender and had a gap of subject-age (average age over visits of no-to-low/heavy drinking, eFigure 1b) less than 6 months. A Ford-Fulkerson algorithm [3] was then applied to select a maximum number of matching pairs. This process resulted in a matched dataset of 78 no-to-low and 78 heavy drinkers.

Participants. Of all the 831 NCANDA participants, 782 (94% of the participants) had at least 2 usable DTI scans by the 5th year of the study, 699 (84%) has at least 3 scans, 588 (71%) had at least 4 scans, 373 (45%) had all 5 scans.

eTable describes the demographics of the NCANDA participants used in the study. The whole cohort is composed 451 participants who had at least 2 usable DTI scans by the 5th year and were labelled as no-to-low drinking (adjusted Cahalan [4] = 0) throughout the study or as heavy drinking (adjusted Cahalan ≥ 2) for at least two consecutive visits. Two age-sex matched groups of 78 no-to-low and 78 heavy drinkers were selected from the whole cohort. 63 out of the 160 heavy drinkers were classified as transitioners as they remained no-to-low drinking for at least two visits before initiating heavy drinking.

MRI Preprocessing. The structural and diffusion data of all NCANDA participants were preprocessed using the publicly available longitudinal NCANDA pipeline [5]. Skull stripping and aligning with the SRI 24 atlas [6] were performed by registering the T1w of each visit to the baseline T1w and registering the baseline to the atlas with ANTS [7]. For each visit, the b0 scan of the DTI sequence was aligned to the T1w MRI by aligning the b0 to the T2w scan via ANTS and aligning the T2w to the T1w via CMTK [8]. Besides skull stripping, the pipeline performed removal of bad single shots, echo-planar structural distortion, Eddy-current distortion correction, fractional anisotropy (FA) estimation by CAMINO [9], and FA skeleton estimation by Tract-Based Spatial Statistics (TBSS) [10]. The average FA value over the whole-brain TBSS skeleton and with respect to the parcellation defined by the Johns Hopkins University (JHU) DTI atlas [11] was computed for each scan and corrected for manufacturer difference based on human-phantom data [5].

Slope Estimation. The group-level DTI trajectory of the 291 no-to-low drinking youths was estimated by a mixed effects model [12], which used a stepwise regression [13] to determine the highest order of the aging effect (eFigure 1a). The model was initialized as a linear function of age (with other covariates) and higher-order terms were successively added until the coefficient was not significantly different from 0 (p-value > 0.05) according to the t-test performed within the GLM. In doing so, the model used a cubic function of age as the fixed effect and incorporated a linear random effect of age (a random intercept and a random slope) for each participant. Confounders including sex, ethnicity, supratentorial volume, pubertal development, socioeconomic status and manufacturer type were considered as covariates in the mixed effects model. For each participant, confounding effects (not including age) were residualized from the FA measures based on the fixed effects estimated within the mixed effects model. To compute the slope measure for each no-to-low drinker, a linear model was fitted between age and residualized FA across all visits (eFigure 1b). For each heavy drinker, the slope was computed with respect to the visits during which the participants engaged in heavy drinking.

eResults. Supplementary Results

Analysis on the Slopes of Transitioners. An Analysis of Covariance (ANCOVA) model compared the slopes among the 291 no-to-low drinkers, the 97 heavy drinkers excluded in the within-subject analysis, and the 63 transitioners before and after drinking onset, while controlling age as a covariate. eFigure 3a indicates that the slopes of the 291 no-to-low drinkers were not significantly different from those of the transitioners prior to drinking onset (95% CI of group difference [-0.0010,0.0002], two tailed $p = 0.09$) but significantly larger than the slopes of transitioners after drinking onset (95% CI of group difference [0.0020,0.0037], $p < 0.001$). On the other hand, the slopes of the 97 heavy drinkers were not significantly different from those of the transitioners after drinking onset (95% CI of group difference [-0.0003,0.0023], two tailed $p = 0.13$) but significantly smaller than the slopes of transitioners before drinking onset (95% CI of group difference [-0.0048,-0.0023], $p < 0.001$).

eFigure 1. Subject-Level and Group-Level Trajectory of FA

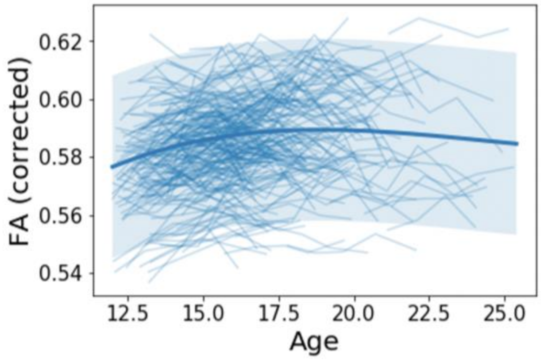

(a)

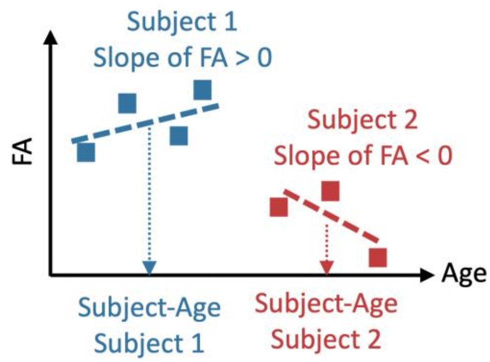

(b)

(a) The group-level developmental trajectory of 291 no-to-low drinking youths; (b) the slope quantifies the developmental change of FA across visits.

eFigure 2. Extension of Figure 2d in the Main Text

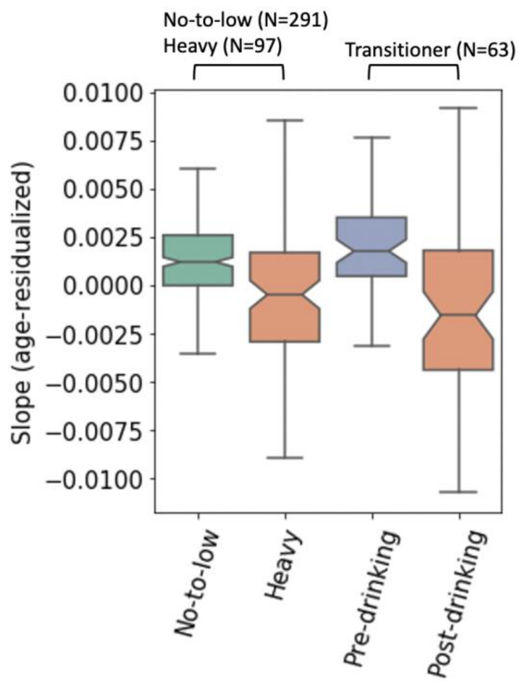

Slopes of the 291 no-to-low drinkers vs. slopes of the 97 heavy drinkers excluded in the within-subject analysis vs. slopes of the 63 transitioners before and after drinking onset.

Estimating Transition Age via Piecewise Linear Model. For each of the 63 transitioners**,** a piecewise linear model [14] was fitted to the residualized FA across visits. The model considered two linear segments and used the `residual sum of squares' algorithm [14] to automatically determine the breakpoint. This breakpoint was compared to the 'actual' age of drinking onset, which was defined as the average age between the two consecutive visits that the participant transitioned from no-to-low to heavy drinking. A paired *t*-test resulted in a two-tailed *p*-value of 0.53, indicating that the data-driven breakpoints (change of slope) were not significantly different from the 'actual' age of transition to heavy drinking.

eFigure 3. Piecewise Linear Regression to Estimate Drinking Onset

Breakpoints of the 63 transitioners estimated by piecewise linear model vs. the actual age of transition from no-to-low to heavy drinking.

eFigure 4. Correlation Between Confounding Variables and Slope of FA

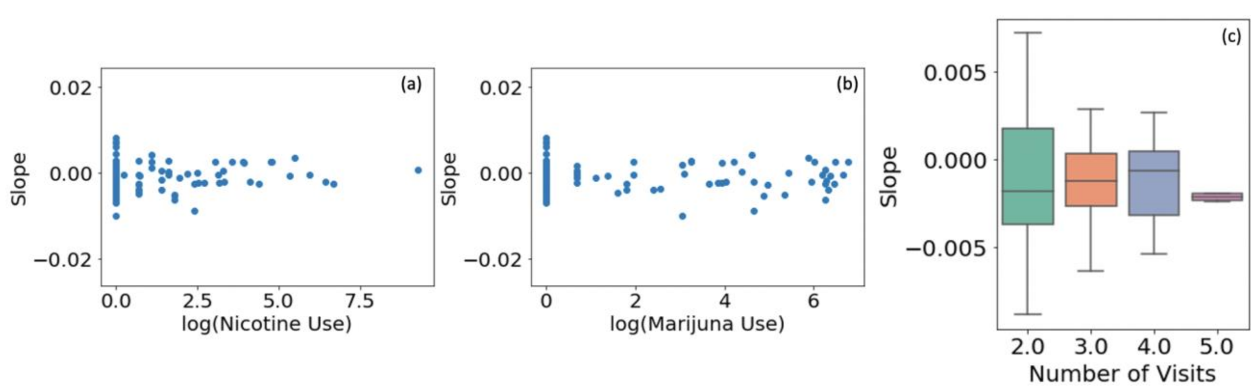

The slope of FA did not significantly correlate with the log of nicotine use, log of marijuana use, or the number of visits of the 156 age-sex-matched subjects (p > 0.1).

Age-alcohol Interaction on the Whole Cohort. On the entire cohort of 451 youth, a general linear model (GLM) examined the subject-age-by-drinking-group interaction on the slope measures with additional covariates being subject-age, sex, and drinking-group. The coefficient associated with the interaction term was statistically significant (two-tailed $p<0.001$).

eFigure 5. Extension of Figure 3b in the Main Text

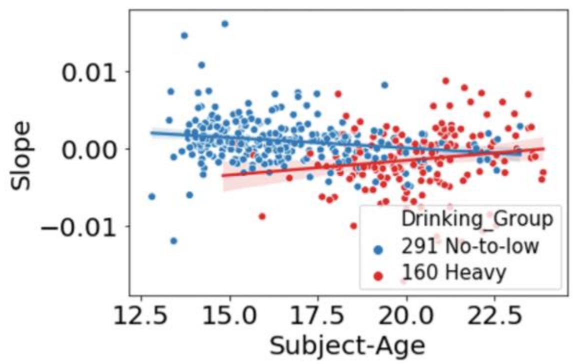

The age-drinking-group interaction on the slope in the 291 no-to-low and 160 heavy drinkers.

Differential Alcohol Effects in Younger and Older Adolescents.

eFigure 6. Extension of Figure 4 in the Main Text

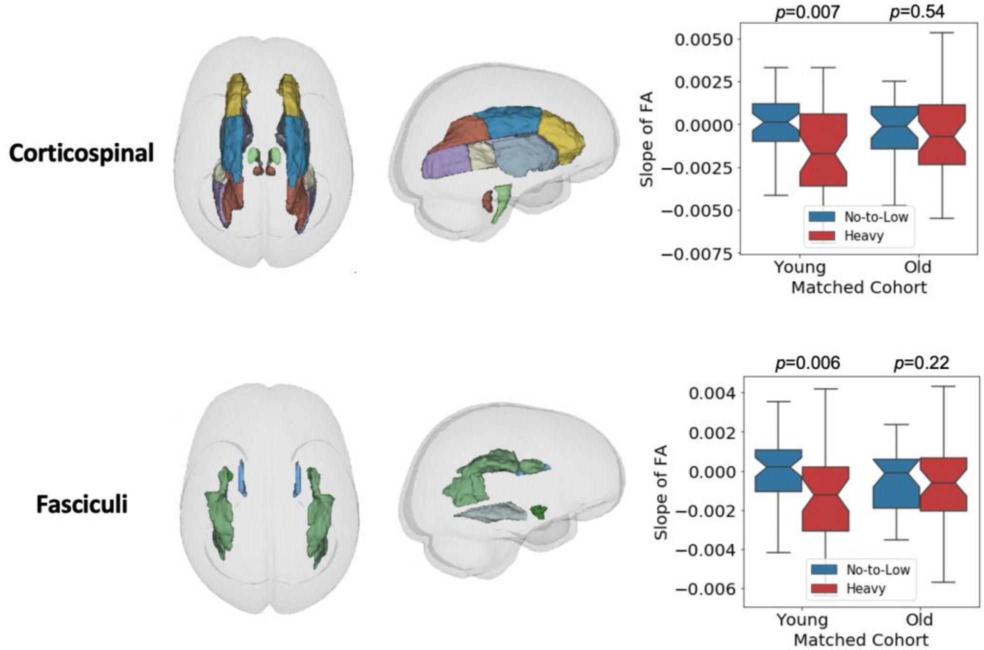

Alcohol effects on the slope within the corticospinal and fasciculi tracts [11] were significant in the younger cohort (age < 19.3 years) but not in the older cohort.

eTable. Demographics of the NCANDA Participants

		Whole Cohort		Matched Cohort		Transitioners	
		No-to-low	Heavy	No-to-low	Heavy	Before Drinking	After Drinking
N		291	160	78	78	63	
Sex (Boys/Girls)		142/149	86/74	40/38	40/38	36/27	
Age (Years)	Boys	16.5±2.2	20.1±1.5	19.3±1.6	19.4±1.5	17.2±1.5	19.5±1.3
	Girls	16.5±2.1	20.5±2.0	19.1±2.0	19.3±2.0	18.5±1.8	20.3±1.9
Scanner (GE/Siemens)		194/97	96/64	42/36	50/28	42/21	
Supratentorial Volume (cm^3)		1313±136	1351±145	1315±141	1353±156	1380±150	
Ethnicity	Caucasian	192	142	57	72	56	
	African-American	54	10	9	3	5	
	Asian	26	4	10	0	1	
	Other	19	4	2	3	1	
Socioeconomic Status		16.6±2.5	17.2±2.5	16.6±2.5	17.2±2.5	17.0±2.2	
Pubertal Development Scale		3.3±0.5	3.7±0.3	3.7±0.3	3.7±0.3	3.5±0.4	3.7±0.3
Substance Consumed During Study	Days of Drinking	0.9±2.1	169.4±130.6	1.7±3.1	171.9±137.0	1.0+1.6	49.3±31.7
	# of Cigarettes	0.17±1.3	127.5±1006	0.3±2.0	203±1423	0.12+4.0	7.1+30.1
	Days of Marijuana Use	1.4±14.4	126.5±262.4	3.5±27	149.5±285.7	0.7+1.7	57.8+95.1

***** Distribution is characterized by mean±std

eReferences

1. Gibbons A. *Algorithmic Graph Theory*. Cambridge University Press; 1985.
2. Rosenbaum PR. Optimal Matching for Observational Studies. *Journal of the American Statistical Association*. 1989;84(408):1024–1032.
3. Ford LR, Fulkerson DR. Maximal flow through a network. *Canadian Journal of Mathematics*. 1956;8:399-404.
4. Pfefferbaum A, Kwon D, Brumback T, et al. Altered Brain Developmental Trajectories in Adolescents After Initiating Drinking. *Am J Psychiatry*. 04 2018;175(4):370-380. doi:10.1176/appi.ajp.2017.17040469
5. Pohl KM, Sullivan EV, Rohlfing T, et al. Harmonizing DTI measurements across scanners to examine the development of white matter microstructure in 803 adolescents of the NCANDA study. *Neuroimage*. Apr 15 2016;130:194-213. doi:10.1016/j.neuroimage.2016.01.061
6. Rohlfing T, Zahr NM, Sullivan EV, Pfefferbaum A. The SRI24 multichannel atlas of normal adult human brain structure. *Hum Brain Mapp*. May 2010;31(5):798-819. doi:10.1002/hbm.20906
7. Avants BB, Tustison NJ, Song G, Cook PA, Klein A, Gee JC. A reproducible evaluation of ANTs similarity metric performance in brain image registration. *Neuroimage*. Feb 1 2011;54(3):2033-44. doi:10.1016/j.neuroimage.2010.09.025
8. Rohlfing T, Maurer CR, Bluemke DA, Jacobs MA. Volume-preserving nonrigid registration of MR breast images using free-form deformation with an incompressibility constraint. *IEEE Trans Med Imaging*. Jun 2003;22(6):730-41. doi:10.1109/TMI.2003.814791
9. Cook PA, Bai Y, Nedjati-Gilani S, et al. Camino: Open-Source Diffusion-MRI Reconstruction and Processing. presented at: 14th Scientific Meeting of the International Society for Magnetic Resonance in Medicine; 2006; Seattle, WA.
10. Smith SM, Jenkinson M, Johansen-Berg H, et al. Tract-based spatial statistics: voxelwise analysis of multi-subject diffusion data. *Neuroimage*. Jul 2006;31(4):1487-505. doi:10.1016/j.neuroimage.2006.02.024
11. Mori S, Wakana S, Nagae-Poetscher LM, van Zijl PCM. MRI Atlas of Human White Matter. *American Journal of Neuroradiology*. 2006;27(6):1384-1385.
12. Laird NM, Ware JH. Random-effects models for longitudinal data. *Biometrics*. Dec 1982;38(4):963-74.
13. Efroymson MA. *Multiple regression analysis*. Mathematical Methods for Digital Computers. Wiley; 1960.
14. Muggeo VMR. Estimating regression models with unknown break‐points *Statistics in Medicine*. 2003;22(19):3055–3071.